

## Electronic Supplementary Information (ESI)

# **An atomistic view of the interfacial structures of AuRh and AuPd nanorods**

**Ruth L. Chantry,<sup>a</sup> Ivailo Atanasov,<sup>b</sup> Wilai Siriwatcharapiboon,<sup>b</sup> Bishnu P. Khanal,<sup>c</sup> Eugene R. Zubarev,<sup>c</sup> Sarah L. Horswell,<sup>b</sup> Roy L. Johnston<sup>b</sup> and Z. Y. Li<sup>\*a</sup>**

<sup>a</sup> *Nanoscale Physics Research Laboratory, School of Physics and Astronomy, University of Birmingham, Edgbaston, Birmingham, B15 2TT, UK. \*E-mail: z.li@bham.ac.uk*

<sup>b</sup> *School of Chemistry, University of Birmingham, Edgbaston, Birmingham, B15 2TT, UK*

<sup>c</sup> *Department of Chemistry, Rice University, Houston TX77005, USA*

### SI.1. Low magnification images of AuPd, AuRh and Au-only nanorods

Figure S1 shows typical low magnification images of Au-only, AuPd and AuRh nanorods. Core-shell segregation is apparent in the majority of the  $\text{Au}_{\text{core}}\text{Pd}_{\text{shell}}$  nanorods in Figure S1(b), whereas similar segregation is not shown in any of the  $\text{Au}_{\text{core}}\text{Rh}_{\text{shell}}$  nanorods in either Figure S1(c) or (d). Figure S1(c) shows the early stages of Rh deposition, predominantly at the corners of the nanorods, contrasting with the thicker Rh coverage in Figure S1(d) and the more rounded appearance of the Au-only seed nanorods of Figure S1(a).

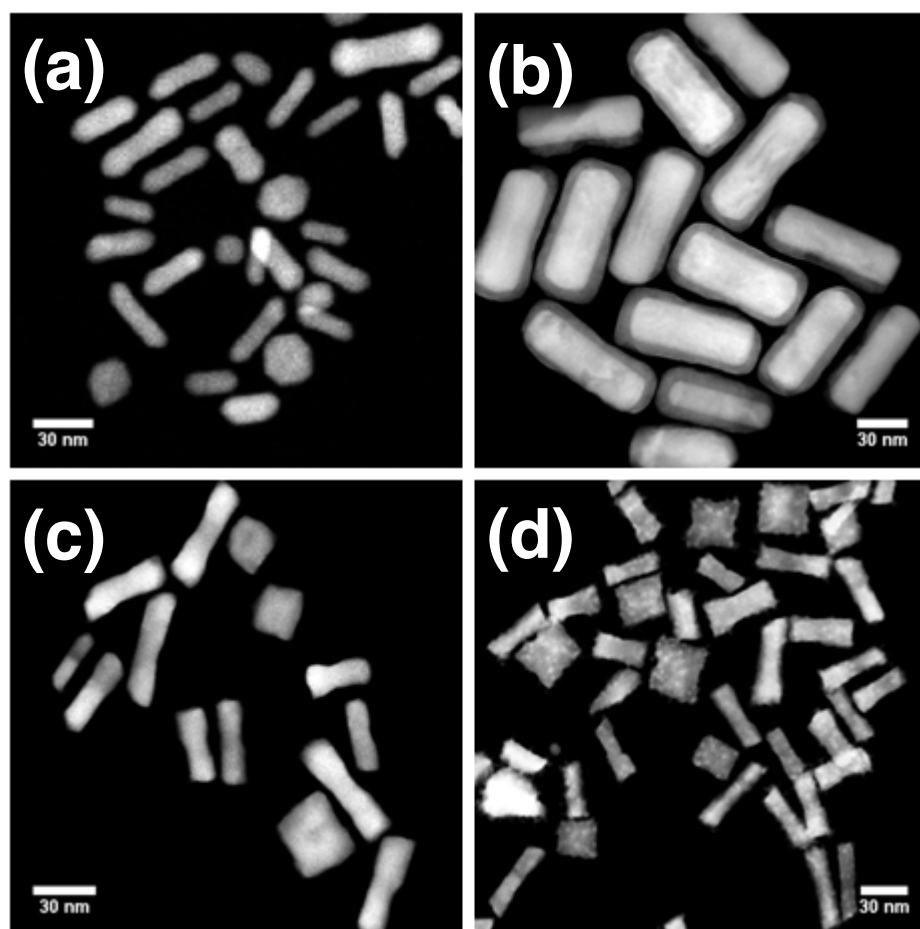


**Figure S1** HAADF-STEM images of (a) the Au-only seed nanorods from the AuRh series of samples, (b)  $\text{Au}_{\text{core}}\text{Pd}_{\text{shell}}$ , (c) and (d)  $\text{Au}_{\text{core}}\text{Rh}_{\text{shell}}$  nanorods with Au:Rh molar ratios of respectively 10:1 and 1:2.

## SI.2. STEM imaging of AuRh nanorod with thick Rh coverage

In Figure S2(a) the mean lattice fringe spacing over Region 1 is 0.19 nm, which corresponds to the [002] lattice spacing for Rh. Closer to the interface, in Region 2, the mean lattice spacing is 0.20 nm, which corresponds to the [002] lattice spacing of Au, despite still being located within the Rh over-growth. Figure S2(b) shows the corresponding simultaneously acquired HAADF image.

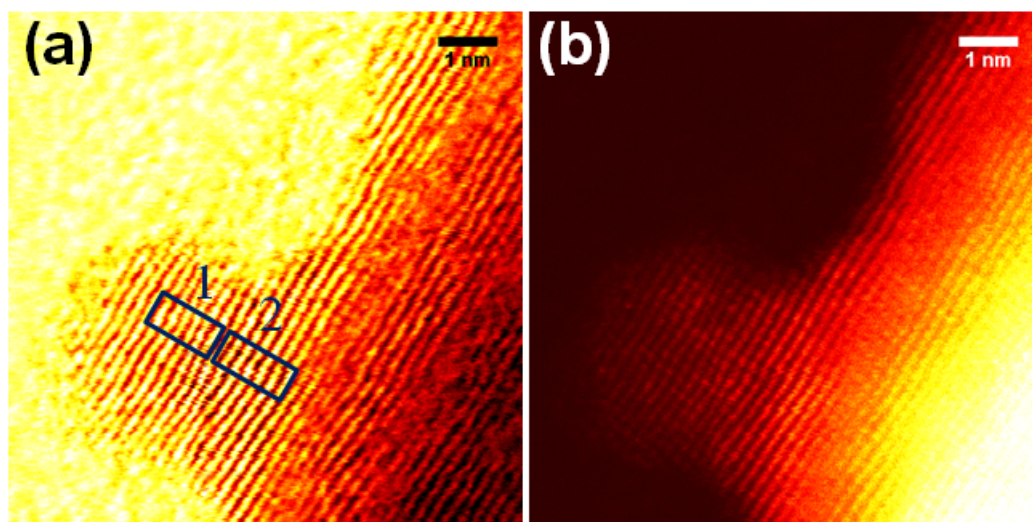


**Figure S2** (a) STEM-BF and (b) STEM-HAADF images of the interfacial region of a  $\text{Au}_{\text{core}}\text{Rh}_{\text{shell}}$  nanorod with thicker Rh coverage.

### SI.3. Molecular dynamics calculations

We have conducted molecular dynamics simulations of the vapour deposition of Au and Pd on planar {100} and {111} Au surfaces, at temperatures between 300 K and 500 K. We have used interatomic potentials based on the second-moment tight-binding approximation.<sup>1</sup> The parameters used are listed in Table S1. The parameter set for the Au-Pd interactions is fitted to bulk elastic constants and experimental mixing enthalpies.<sup>2-4</sup> Those for the Au-Rh system include the Rh-Rh potential from reference 1 and an Au-Au potential separately fitted to surface energies and the hcp-fcc energy difference.<sup>5</sup> The Au-Rh part has been fitted to the miscibility properties of Rh and Au in the bulk. The predicted Au-Rh heats of solutions of impurities are 0.487 eV and 0.668 eV for Rh in Au and Au in Rh, respectively, in accordance with reference 6.

**Table S1:** Parameter sets used for modelling Pd-Au and Rh-Au. Parameter notations correspond to references 1 to 4.

Parameter	Pd-Au <sup>2-4</sup>			Rh-Au <sup>1</sup>		
	Pd-Pd	Pd-Au	Au-Au	Rh-Rh	Rh-Au	Au-Au
A (eV)	0.1715	0.2764	0.2096	0.062891	0.120341	0.129097
$\xi$ (eV)	1.7019	2.0820	1.8153	1.660162	1.516005	1.522199
p	11.000	10.569	10.139	18.450	9.529	12.500
q	3.7940	3.9130	4.0330	1.8670	1.7893	3.5500
$r_0$ (Å)	2.7485	2.8160	2.8840	2.6891	2.7867	2.8843

In all cases the Au substrates consist of 6 crystallographic planes. The atomic positions of the lowest plane were fixed to the bulk lattice constant at the given temperature, thus taking into account the thermal expansion of Au predicted by the atomic potentials. Periodic boundary conditions in the ( $x$ ,  $y$ ) directions were applied. We first equilibrated the Au substrate to the given temperature and then deposited Pd or Rh atoms at random ( $x$ ,  $y$ )

positions at a rate of 1 atom/ns. The Nosé-Hoover thermostat with  $Q = 0.55 \times 10^{-25}$  eV s<sup>2</sup> was applied<sup>7</sup> in order to keep the sample temperature constant during the deposition process.

We observe Rh growth forming surface clusters on both surface orientations, consistent with Au/Rh immiscible behaviour in bulk. The surface diffusion rate of Rh adatoms on the {100} substrate was just high enough to observe the initial stages of the formation of surface clusters at temperature 300 K for the deposition rate applied but the Rh atoms were much more mobile on the {111} surface as a result of the lower adatom coordination number. In comparison our results show that Pd has a tendency to wet the Au surfaces. We observe substitutions of Pd adatoms and surface Au atoms on the {100} orientation even at 300 K; however, on the {111} Au surface Pd follows ideal layer-by-layer growth.

One possible scenario to explain experimentally observed sharp Pd/Au interfaces is that the rapid formation of an evenly distributed Pd layer kinetically traps the system in a metastable state and prevents Au atoms emerging onto the surface. In contrast, the formation of Rh clusters on the Au surface may allow a route for Au atoms to migrate and attach themselves to the Rh clusters, eventually being buried by further Rh deposits.

In order to test this hypothesis for the observed interfacial structure, we have also conducted a simulation which added several Au atoms to the substrate after 0.5 monolayer coverage of Rh deposited on Au{111}. The system was then annealed for another 20 ns at 300 K. In this simulation, when annealed at 300 K we observed the new Au adatoms moving to the edge of the Rh cluster. At 400 K, some Au atoms were seen to climb on top of these Au atoms. Finally, at 500 K, we observed Au adatoms climbing onto the Rh clusters. This behaviour shows a preference for low-coordinated Au atoms to bond to Rh, rather than Au, which is consistent with stronger Au-Rh binding than Au-Au binding.

We note that the conditions of our MD simulations are far from the real conditions of sample preparation, which are too complex to be easily modelled. These results therefore report general trends in the deposition processes, governed by the internal properties of the AuPd and AuRh systems alone, and are not intended to give a full explanation of the systems we observe experimentally.

#### SI.4. Sample synthesis

##### *AuRh*

The Au seed NRs were synthesized using the method of Nikoobakht and El Sayed,<sup>8</sup> as modified by He *et al.*<sup>9</sup> 10.0 mL 0.1 M cetyl trimethyl ammonium bromide (CTAB) aqueous solution was mixed with 100  $\mu$ L 0.025 M HAuCl<sub>4</sub>, with the addition 0.6 mL of ice-cold 0.01 M of NaBH<sub>4</sub>. The seed solution was stirred vigorously for 3 minutes, kept at room temperature and used within 2-5 hours of preparation. The Au NR growth solution was made with 100 mL 0.1 M CTAB, 2.0 mL 0.025 M HAuCl<sub>4</sub>, 1 mL 0.01 M of AgNO<sub>3</sub> and 1 mL 0.1 M ascorbic acid, also prepared at room temperature. 240  $\mu$ L of seed solution was added to the growth solution with no further stirring or agitation.

Rh was deposited onto the Au NRs by reducing a 0.002 M aqueous solution of sodium hexachlororhodate (III) on to the Au NRs. 6 mL Au NR solution was centrifuged at 6000 rpm for 1 hour, to remove excess CTAB and nanospheres. The supernatant was removed using a pipette and the NRs were re-dispersed in 0.5 mL ultrapure water. The molar ratio of Au:Rh was varied by mixing 0.5 mL of Au NR solution with different volumes of 0.002 M Na<sub>3</sub>RhCl<sub>6</sub>·12H<sub>2</sub>O reagent (0.15, 0.643, 1.5, and 3.0 mL), giving samples with molar ratios Au:Rh of 10:1, 7:3, 1:1 and 1:2. 1 mL 0.2 M ascorbic acid was added and the total volume of each sample was adjusted to 4.5 mL. The mixture was stirred for 2 h at 40 °C. Water purified with a MilliQ Gradient A10 system was used throughout.

##### *AuPd*

Gold nanorods were prepared on 500 mL scale using a modified seed-mediated method. 364 mg CTAB was dissolved in 5 mL of water at 30 °C. In a separate vial, 1 mg HAuCl<sub>4</sub>·3H<sub>2</sub>O was dissolved in 5 mL water. These two solutions were mixed together before 0.6 mL 0.01M ice-cold aqueous solution of NaBH<sub>4</sub> was introduced in one step with vigorous stirring (1200 rpm). The colour changed from greenish-yellow to dark brown as the mixture was stirred for 2 minutes. Growth solution was prepared by dissolving 18.22 g CTAB (slight heating is necessary) and 8.5 mg AgNO<sub>3</sub> in 250 mL of water. After 10 minutes, 250 mL of aqueous solution of HAuCl<sub>4</sub>·3H<sub>2</sub>O (prepared separately by dissolving 98.5 mg HAuCl<sub>4</sub>·3H<sub>2</sub>O in 250 mL H<sub>2</sub>O) was added to the mixture of CTAB and AgNO<sub>3</sub>. After an additional 3

minutes, 3.6 mL of 0.08 M solution of ascorbic acid was added to the above mixture. The flask was hand-stirred until the mixture became colourless (typically 3-5 seconds). Next, 0.8 mL of seed solution was added all at once to the growth solution and the mixture was stirred for 15 seconds. The flask containing the growth solution was then placed into an oil bath at 27 °C and kept without stirring. A reddish-brown colour slowly developed within the first 10-15 minutes. In order to convert the remaining Au(I) ions to metallic gold 5 mL 0.1 M solution of ascorbic acid was added to 500 mL solution of Au NRs. The colour changed from brown to dark brown/red within 10 min and the reaction mixture was kept undisturbed for 2 h.

In a separate flask, a stock solution of  $1.974 \times 10^{-3}$  M Pd(II) was prepared by dissolving 35 mg of PdCl<sub>2</sub> in 10 mL 0.2M HCl and stirring for 2-3 hour. After the complete dissolution of PdCl<sub>2</sub>, the solution was further diluted with DI water up to 100 mL. Then 17 mL of  $1.974 \times 10^{-3}$  M solution of PdCl<sub>2</sub> was added to the Au NRs solution and the reaction mixture was left undisturbed for 12 h at 30 °C. Addition of another 34 mL of  $1.974 \times 10^{-3}$  M solution of Pd (II), followed by 10 ml of 0.0788 M ascorbic solution was then carried out, which results in the formation of a 10-12 nm Pd shell on the AuNRs.

## REFERENCES

- [1] F. Cleri, V. Rosato, *Phys. Rev. B* **1993**, *48*, 22–33
- [2] F. Baletto, R. Ferrando, A. Fortunelli, F. Montalenti, C. Mottet, *J. Chem. Phys.* **2002**, *116*, 3856–3863
- [3] F. Pittaway, L.O. Paz-Borbón, R.L. Johnston, H. Arslan, R. Ferrando, C. Mottet, G. Barcaro, A. Fortunelli, *J. Phys. Chem. C* **2009**, *113*, 9141–9152
- [4] R. Ismail, R.L. Johnston, *Phys. Chem. Chem. Phys.* **2010**, *12*, 8607–8619
- [5] R. Ismail, R. Ferrando, R.L. Johnston, *J. Phys. Chem. C* **2013**, *117*, 293–307
- [6] H. Okamoto, T.B. Massalski, *Journal of Metals* **1984**, *36*, 57–57
- [7] P. H. Hünenberger, in *Advanced Computer Simulation*, eds. C. Holm and K. Kremer, Springer: Berlin, 2005, vol. 173, pp. 105–149.
- [8] B. Nikoobakht, M.A. El-Sayed, *Chem. Mater.*, **2003**, *15*, 1957-1962
- [9] W. He, X. Wu, J. Liu, K. Zhang, W. Chu, L. Feng, X. Hu, W. Zhou, S. Xie, *J. Phys. Chem. C*. **2009**, *113*, 10505-10510